DESIGN CHARACTERISTICS OF THE K=800 SUPERCONDUCTING CYCLOTRON AT M.S.U.*

F. Resmini, G. Bellomo, E. Fabrici, H.G. Blosser, and D. Johnson

Introduction

Design work on the proposed K=800, K_F=400, superconducting cyclotron at MSU has progressed to the point where overall machine characteristics are firmly established. The main purpose[1] of the machine is to serve as a booster for the K=500 cyclotron, now under construction. In this respect, let us recall that the design goal is to achieve maximum beam energies of 200 MeV/n for fully stripped light ions, and typically 30-40 MeV/n for heavy ions like uranium. Energy variability down to about 50 MeV/n and 4-5 MeV/n, again for light and heavy ions respectively, is also required, the rationale for these values being that to ensure some overlap with beam energies delivered by the K=500 on a stand-alone mode.

Such an extreme range of beam energies, from very relativistic to non relativistic ones, demands a careful analysis of the intrinsic physics of the machine. Coupling to the first cyclotron, with the associated problems of beam injection and definition of the operating modes of both cyclotrons, is also a complex topic, and has indeed a number of consequences on the machine characteristics.

At this stage we believe that all major topics have been explored in sufficient detail so as to produce a consistent design. In the process, some unexpected findings led us to introduce a few unusual features, and it is the purpose of this paper to discuss the rationale behind them. For the sake of clarity, however, we shall first review the overall design as it stands now, turning thereafter to a detailed analysis of the single issues.

Outline of the Machine Design

A summary of the main cyclotron parameters is given in Table I, while a schematic horizontal layout and a vertical section are presented in Figs. 1 and 2. Choice of the pole radius, minimum hill gap, and sector spiral constant was mainly determined by the axial focussing requirements for 200 MeV/n fully stripped ions. A careful analysis of a number of different configurations indicated that the 41" pole radius was the minimum possible, and it has indeed been associated with a tight spiral and a hill gap of 2.5". In fact, a gap of 3" would already require, for the same spiral, a pole radius of 44"-45" at least. Average field B(r), ν_z and phase are presented as a function of radius in Fig. 3 for two examples of 200 MeV/n and 20 MeV/n beams, showing that the present configuration meets all acceleration requirements.

Table I. Main K=800 parameters.

Pole radius = 41"
Outer hill radius = 42"
No. of sectors = 3, 46° wide
Spiral constant = 1/13 rad/inch
Minimum hill gap = 2.5"
Maximum valley gap = 18"
Minimum-maximum operating fields = 30-50 kG
Yoke height = 117"
Yoke inner and outer diameters = 118"-174"
Total iron weight (poles included) ≃ 260 tons
R.F. frequency range = 9-32 MHz
Harmonic operating modes = 1st, 2nd
Peak dee voltage = 200 kV
R.F. power per dee < 150 kW
No. of trim coils = 22
Maximum total trim coil power ≃ 60 kW

Two peculiar features of the sector geometry are apparent from Fig. 1:

a. A counterclockwise-clockwise behaviour of the spiral, with a transition radius at about 15", which is required for stripping the injected particles in a hill. A detailed discussion of this aspect of the design is given in Ref. 2.

b. A radial cut of the profile from a radius of 40.8" to 42". This, as discussed in detail below, is needed to reduce ν_z values in the extraction region, thus avoiding a dangerous intrinsic resonance.

A central hole of 7" diameter is provided for insertion of stripping foil position mechanism. Dee stems are inserted through 13" diameter holes at a radius of 31". Preliminary R.F. engineering studies indicate that, for the required 9 to 32 MHz range, the short circuit will have to move between 60" and 240" from the median plane, and therefore outside the yoke. It is anticipated that in this region the outer coaxial will be 18" diameter, and the inner one 8" diameter. The power figure quoted in Table I should be regarded at this stage as an upper limit.

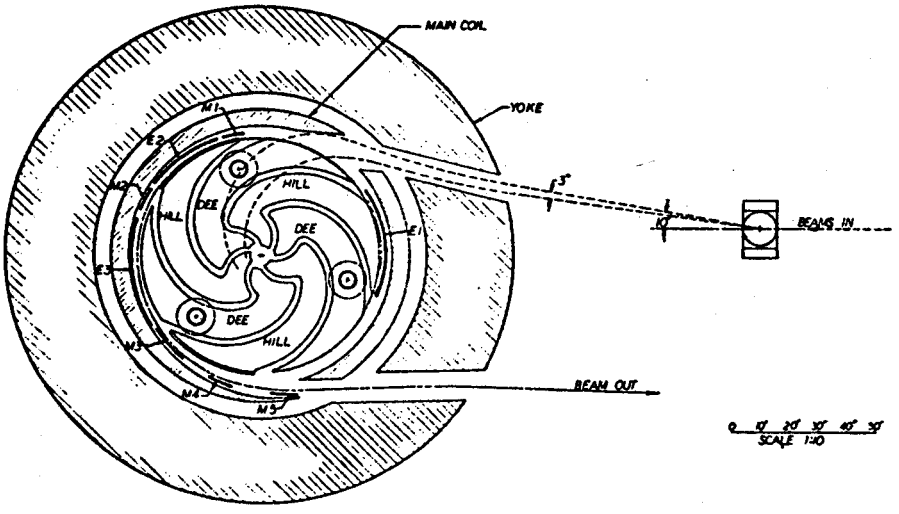

Fig. 1. Schematic layout of the K=800.

*This material is based upon work supported by the National Science Foundation under Grant No. Phy 78-01684.

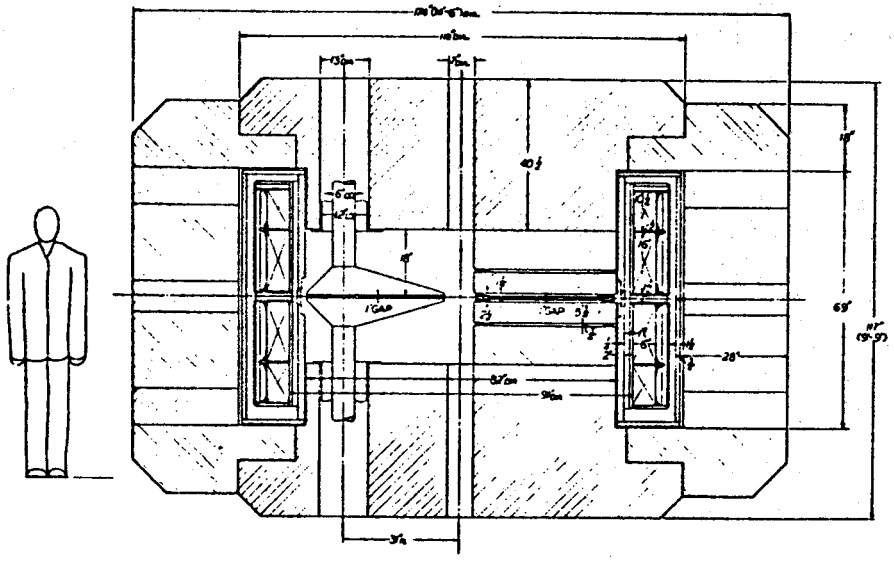

Fig. 2. Section through the magnet of the K=800.

Table II. Coil parameters

Inner coil radius = 45.5"
Outer coil radius = 51.5"
Coil total height = 26.5"
Coil splitting: two sections
Height of section closer to the median plane = 16"
Minimum coil distance from median plane = 1.5"
Maximum current density = 3500 A/cm^2
Ampereturns at maximum current = 7.2 x 10^6
Conductor: Nb-Ti, to be selected
Cryostat inner radius = 41.25"
Cryostat outer radius = 58.25"
Cryostat total height = 68"

Main coil parameters are listed in Table II, and the coil cross section is sketched in Fig. 2. Since a detailed report of the method which led to the coil design is given in Ref. 3, we shall just note here that two section splitting of the coils has been chosen. The larger section is the one closer to the median plane, with a fractional height equal to 0.6 of the total height. This design effectively reduces the total maximum trim coil power needed throughout the cyclotron operating range to about 60 kW for 22 trim coils. The latter, as schematically shown in Fig. 2, have a construction scheme similar to that of the K=500 cyclotron,[4] i.e. they are wrapped around the hills with 2 layers, of 5 turns each, of 1/4" x 1/4" square conductor. Maximum current in each trim coil will be 300 A.

As shown in Fig. 1, extracted and injected beams run almost parallel outside the machine. This turned out to be the only practical scheme, since injection has to be through a valley with beams converging to a common point located about 150" from the cyclotron center.[2] Matching to all required injection paths can be obtained by 3° steering at this point. On the other hand, extraction requires three deflectors and five magnetic channels, over an azimuthal range of 328°, as shown in Fig. 1. Compatibility between injection and extraction leads thus to the present choice.

We turn now to a discussion of the most interesting aspects of the machine operation.

Beam Acceleration

The appearance of the ν_z=1.5 stopband, at radii around 41", was quickly recognized. Its onset is due to the simultaneous presence of a strong alternating gradient effect due to the spiral, and the fast fall-off of the fringing field. Since the stopband is impassable, extraction has to take place before then. However, acceleration runs uncovered the presence of another resonance, the $\nu_R+2\nu_z=3$ (three being the number of the sectors) which is reached well before the ν_z=1.5 stopband. This is shown in the operating (ν_R,ν_z) diagram of Fig. 4, both for 200 MeV/n and 20 MeV/n beams. Existence of such a resonance has been known for a long time,[5] although the conditions for its onset probably never materialized in a three-sector machine. This resonance being of the third order in the Hamiltonian, and intrinsic, it is very nearly impassable. Effects on the axial motion can be seen in Fig. 5 for a perfectly centered beam (curve 1) and two beams where a precessional radial oscillation has been excited by a field first harmonic of amplitude 4 and 6 Gauss. Since traversal of the ν_R=1 resonance occurs well before the $\nu_R+2\nu_z=3$ resonance, it is quite obvious that the latter cannot be crossed.

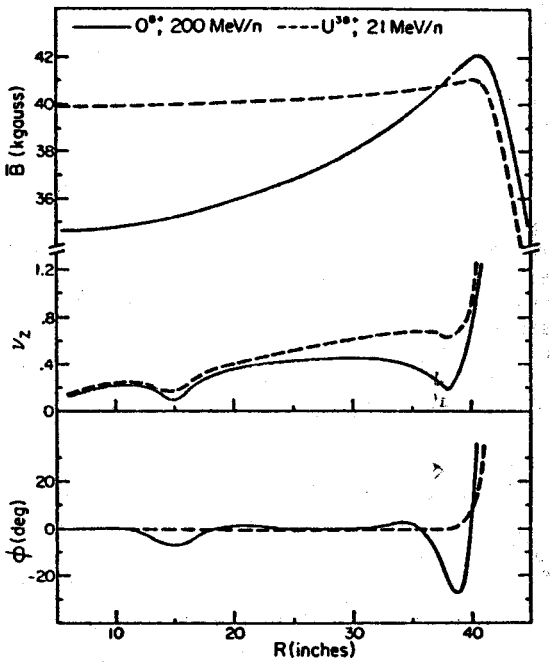

Fig. 3. Average field, ν_z and phase for 200 MeV/n and 20 MeV/n ions.

Analysis of the effective field index experienced by a particle along the equilibrium orbit, as shown in Fig. 6, curve 1, demonstrates that the simultaneous presence of the rapidly decreasing fringing field and the alternating gradient effect due to the spiral is again responsible for the high ν_R and ν_z values. On the other hand, extraction before the resonance is

hardly possible in this configuration since, as seen in Fig. 4, the maximum ν_R value one can reach is about .9.

Radial cuts of the hill profile were therefore tried, to reduce the alternating gradient effect, since the fringing field fall-off can hardly be influenced. This technique proved successful, as shown by curves 2 and 3 of Fig. 6. The main effect of the radial cuts is to push the operating plot, for the same values of ν_z, towards smaller values of ν_R, which is precisely what one wants in order to make extraction easier. We finally settled upon a radial cut from 40.8" to 42", producing the (ν_R,ν_z) diagram seen in Fig. 7. The new distance from the ν_R=1 line can be compared with that of Fig. 4, and extraction is now possible at a ν_R value of about .8.

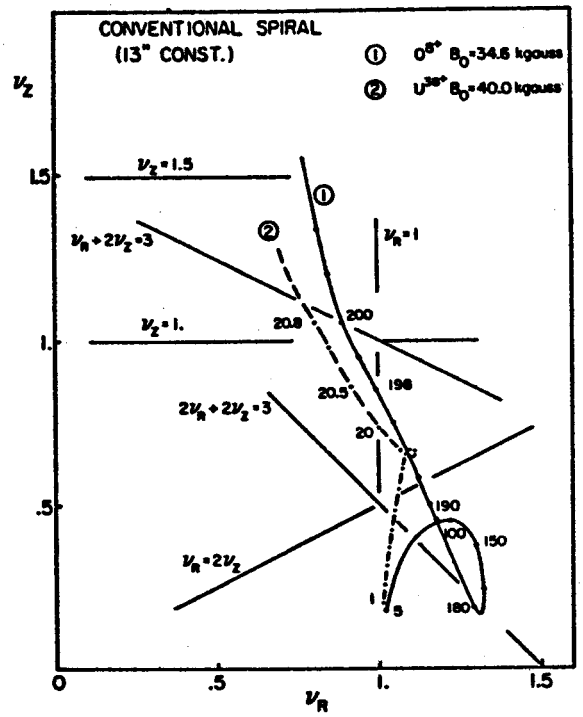

Fig. 4. Operating (ν_R,ν_z) plot for 200 MeV/n and 20 MeV/n ions with a conventional spiral.

The only other resonance present in Fig. 7, which is not usually considered in conventional AVF cyclotrons, is the $2\nu_R+2\nu_z=3$. This, however, is a fourth order resonance; and computer runs established that radial oscillations as large as 0.3" can be easily tolerated. As for the coupling resonance $\nu_R=2\nu_z$, the fact that it is traversed before the ν_R=1 resonance is indeed favourable, and radial amplitudes of .2" can be tolerated.

The appearance of the $\nu_R+2\nu_z=3$ resonance and its consequences led us to analyse very carefully the entire operating range of the cyclotron in the $(B_o,Z/A)$ space. In fact, it can be expected that at low magnetic field values the corresponding flutter increase would push ν_z to values high enough to hit the resonance at radii several inches before any reasonable extraction radius. This actually happens, as can be seen in a straightforward way in Fig. 8 for a Z/A value of accelerated particles equal to 0.5. For low enough central field values, like 25 and 27.5 kG, the resonance is in fact crossed at radii as low as 36", thus effectively prohibiting beam acceleration beyond this radius.

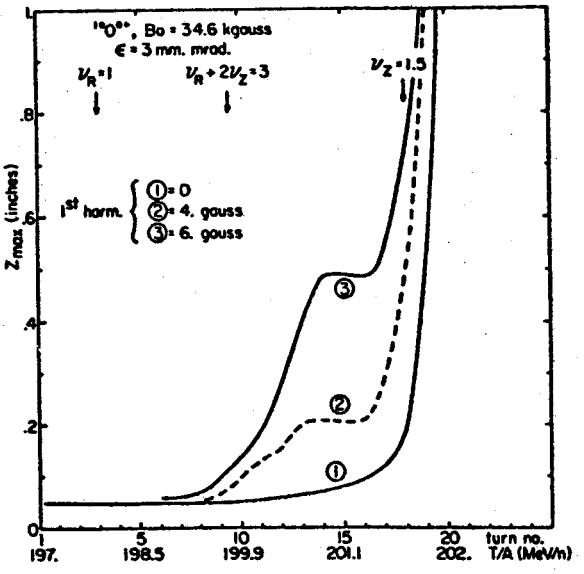

Fig. 5. Axial envelope of accelerated beam. Behavior of a centered beam (1) and of beams for which a precessional oscillation has been excited (2,3) are presented.

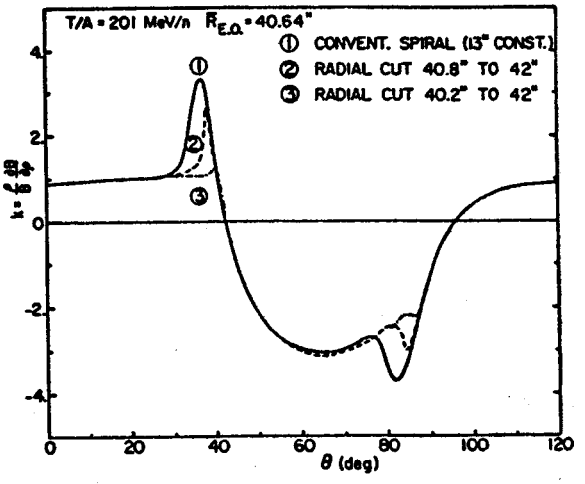

Fig. 6. Effective field index experienced by particles on equilibrium orbit (see text for details).

A number of similar calculations established that in the $(B_o,Z/A)$ plane there exists a limiting line whose equation is approximately

$$B_o\ (kG) = 35. - \frac{5}{.4}\ Z/A$$

which prevents cyclotron operation below its boundary. Consequences of this finding will be seen presently.

Coupling to the K=500 - Operating Modes

Determining the appropriate coupling modes between the two cyclotrons in order to meet design goals has proved a complex matter. Coupling of the two cyclotrons on the basis of equal R.F. acceleration frequencies obeys the following relations:

$$\frac{\beta ex_2}{\beta ex_1} = \frac{Rex_2\ h_1}{Rex_1\ h_2} \qquad (1)$$

hence

$$\frac{T_2/A}{T_1/A} \simeq \left(\frac{Rex_2\ h_1}{Rex_1\ h_2}\right)^2 \qquad (2)$$

$$\frac{Z_2\ h_2}{Z_1\ h_1} = \frac{Bo_1}{Bo_2} \qquad (3)$$

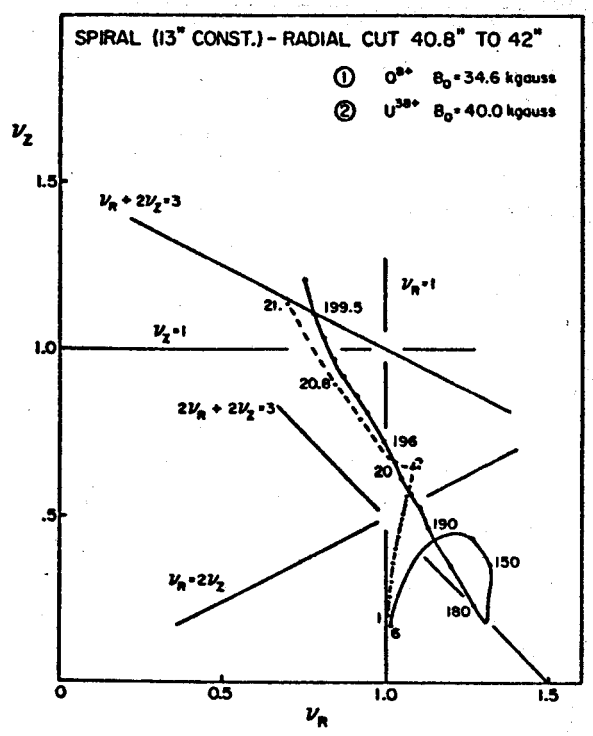

Fig. 7. Operating (ν_R,ν_z) plot with a radial cut in the spiral profile from 40.8" to 42". Same ions and fields as Fig. 4.

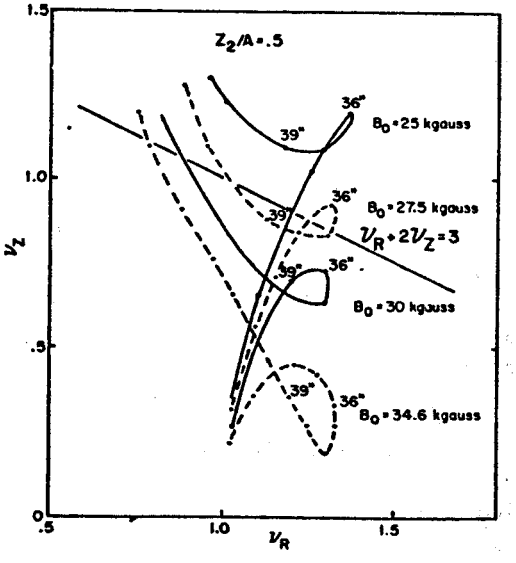

Fig. 8. Operating (ν_R,ν_z) plot for an ion with Z_2/A=.5 at different center field levels.

where T/A, βex, Rex, h, Z, and B_o are the extraction energy, particle velocity, extraction radius, harmonic number, charge state, and center field value of the first cyclotron (K=500) or the second cyclotron (K=800) according to the subscript. The harmonic coupling ratio h_1:h_2 (HCR) is therefore of paramount importance in determining the actual operating parameters.

The particle energies allowed for both machines, according to (1), are presented in Fig. 9 for all harmonic modes. It is seen that because of R.F. limits only HCR of 3:1, 4:1, or 5:1 can be considered for the high energy range, 4:2, 5:2, and 7:2 being available for the low energies. Overlap can occur in the 18 MeV/n to 60 MeV/n range.

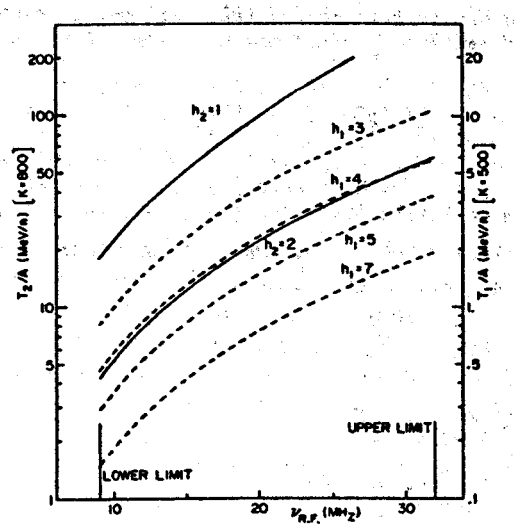

Fig. 9. Energy in MeV/n for both cyclotrons as a function of R.F. frequency for different harmonic modes.

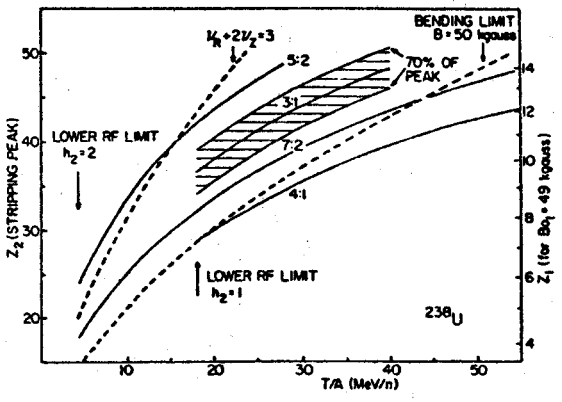

Fig. 10. Most probable charge state after stripping, for uranium, as a function of final energy. See text for details.

The appropriate coupling mode must then be studied for every single ion, keeping in mind the following requirements:

a. for the first cyclotron, the lowest possible harmonic number, h_1, and charge state, Z_1, should always be preferred for obvious beam intensity reasons.

b. The charge state ratios Z_2/Z_1, or stripping ratio, should not only obey (3), but also correspond to the peak, or be very close to the peak, of the stripping distribution for any given injection energy.

c. Bending, focussing, and resonance limits have to be strictly observed.

How this study is actually done can be seen in Fig. 10 for the case of uranium. The most probable charge state Z_2, after stripping, is plotted as a function of the final energy for all possible harmonic coupling ratios. For the case of HCR 3:1 the band corresponding to 70% of the peak intensity is also shown, to give an idea of the limits posed by requirement (b). The scale on the right refers to the minimum charge state Z_1 allowed in the first cyclotron, according to a field center value of 49 kG, and can be used for every HCR curve. Also indicated are the $\nu_R+2\nu_Z=3$ limit and the bending limit for 50 kG at extraction radius. One

sees immediately that the 3:1 mode is the lowest possible over the 18 to 40 MeV/n range, the upper limit coming from charge state $Z_1=14^+$ in the first machine.

Even higher energies are possible, up to 50 MeV/n, using the 7:2 mode. One must allow departure from the maximum stripping intensity, because of the bending limit in the second cyclotron, but still within 70% of the peak value. At energies lower than 18 MeV/n, where the second harmonic must be used for the K=800, the 7:2 mode is always possible, while the 5:2 mode can only be used by shifting off the peak intensity, because of the resonance.

These curves can be transformed into $(B_o, Z_2/A)$ diagrams, as shown in Fig. 11, where for each energy in MeV/n the limits within 70% of the peak intensity are drawn for every HCR. In this diagram one can appreciate not only the necessary range of magnetic fields, but also how and in which range the energy can be varied continuously by keeping a constant Z_2/A value and just varying the magnetic field.

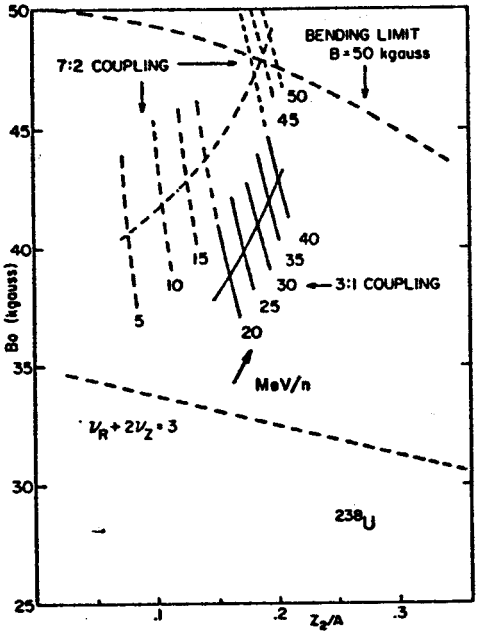

Fig. 11. Operating $(B_o, Z_2/A)$ plot for uranium. For every HCR the center line refers to the peak charge state, and crosses constant T/A lines.

Similar analyses have been made for a number of ions throughout the periodic table. When all these results are put together, one obtains the overall operating diagram in the $(B_o, Z_2/A)$ plane shown as a gray area in Fig. 12. The boundaries of the operating region are given in a self-explanatory way on the figure itself. Also shown are the operating lines for a number of representative ions, and HCR=3:1 and 7:2, corresponding to the most probable charge state after stripping.

The same analysis also determines, for each ion and HCR, the limits of the stripping ratio, Z_2/Z_1. They are presented for HCR=3:1 and for ^{63}Cu, ^{122}I, and ^{238}U, in Fig. 13 as a function of the final energy per nucleon. The dashed lines correspond to constant charge state Z_1 and, for each energy, to the most probable charge state Z_2. The upper limit on Z_2/Z_1 is then given by the bending limit of the first cyclotron. The lower line is instead a possible limit for the continuous transition from one charge state Z_1 to the next one, while keeping Z_2 at the value for peak stripping intensity. It is seen from Fig. 13 that:

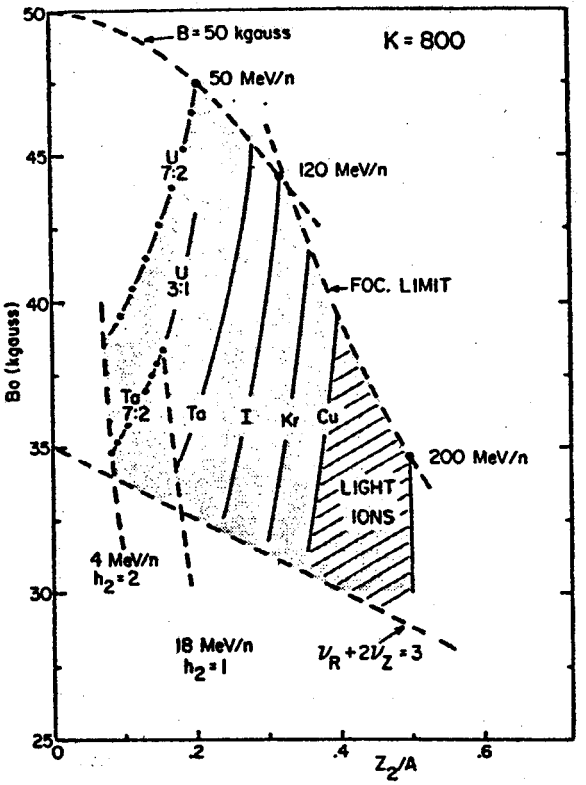

Fig. 12. Overall $(B_o, Z_2/A)$ operating diagram for the K=800.

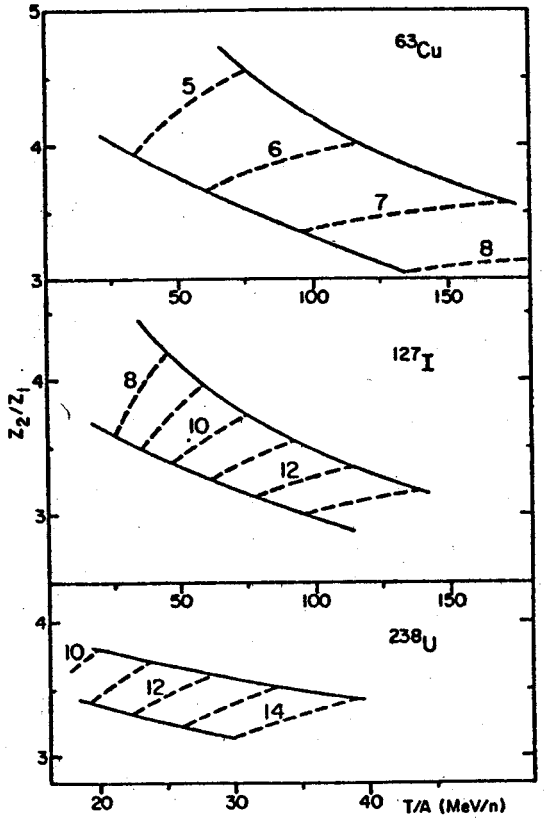

Fig. 13. Stripping ratios as a function of energy for HCR=3:1 and different ions. See text for details.

- practically the same range of Z_2/Z_1 applies for every ion.
- Z_2/Z_1 must decrease as a function of energy.
- henceforth the injection must accomodate a fairly large range of stripping ratios[2] for proper coupling of the two cyclotrons.

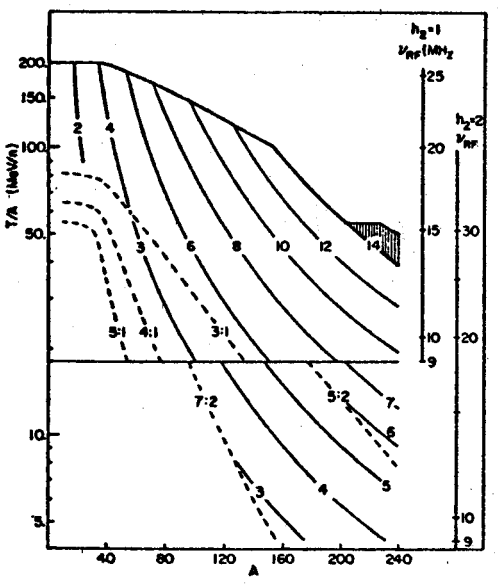

Fig. 14. T/A in MeV/n vs. ion mass number.

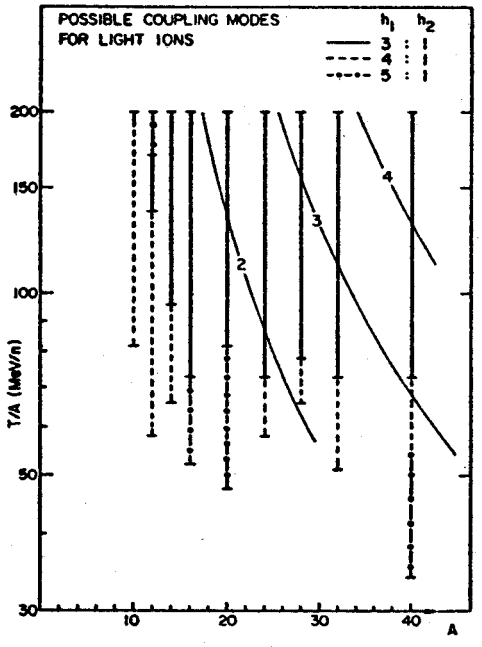

Fig. 15. T/A in MeV/n for light ions.

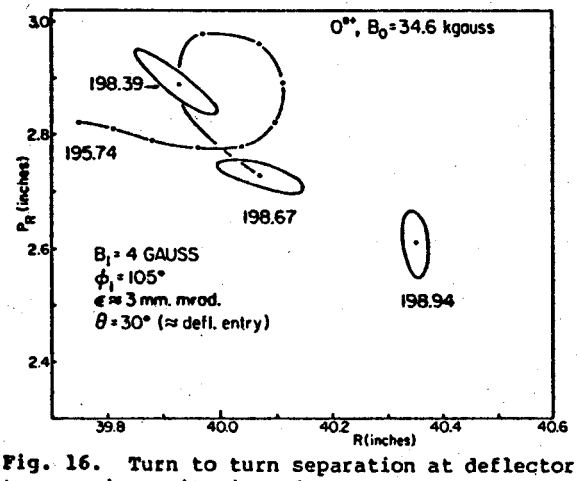

Fig. 16. Turn to turn separation at deflector entrance via excitation of ν_R=1 resonance.

In the customary T/A vs. A plane, the machine performance is illustrated in Fig. 14. The limits for the various HCR, as defined by the $\nu_R+2\nu_z=3$ resonance, are shown as dashed lines. At 18 MeV/n, i.e. 9 MHz, there is the lower limit for first harmonic operation. The bending limits of the K=500 are also shown for a number of charge states Z_1 and, for $Z_1=14^+$, they determine the machine characteristic for $A\geq150$. The dashed region for $A\geq200$ corresponds to the possible use of the 7:2 HCR as discussed above for uranium. The focussing limit, K_F=400, defines the maximum energies for A<150. An enlarged scale diagram is given for light ions in Fig. 15, details being noted on the figure in a self explanatory way.

From this analysis the following main conclusions can be drawn:

- The 3:1 HCR can and should be used over most of the high energy range. The presence of the $\nu_R+2\nu_z=3$ resonance does, however, severely restrict its use at low energies for light and medium ions, where a switch to 4:1 or 5:1 mode is compulsory. Likewise, the 2:1 mode is really not interesting since its limits are obviously higher than for the 3:1 mode.
- For energies below 18 MeV/n, the 5:2 mode has a very narrow range in terms of T/A vs. A, and the 4:2 mode is therefore not practical. The 7:2 mode can instead be used over a very wide range. Should energies below 18 MeV/n be desired for mass numbers below 100, one should recur to even higher harmonic modes in the first cyclotron. Their practical feasibility has not, however, been investigated yet.

As for the operating region of the first cyclotron in the $(B_{o1}, Z_1/A)$ plane, we have found that Z_1/A should range from 0.02 to 0.15, with magnetic field values spanning from 30 to 49 kG.

Beam Extraction

Extraction studies have been concentrated so far on a careful analysis of the 200 MeV/n case. The extraction scheme, as shown in Fig. 1, consists of three deflectors positioned in two consecutive hills and a valley, and five magnetic channels. The latter are of the passive type, i.e. saturated iron bars, and therefore produce both a negative bias field and a radially focussing gradient. Parameters for all elements as used in the extraction of 200 MeV/n beams are given in Table III.

Table III. Extraction scheme characteristics.

Element	Δθ (deg.)	E. field (kV/cm)	-ΔB (kG)	∂B/∂x (kG/inch)
E_1	58°	140.	---	---
M_1	10°	---	2..	5.8
E_2	36°	140.	---	---
M_2	12°	---	2.	5.8
E_3	50°	140.	---	---
M_3	18°	---	2.	5.8
M_4	10°	---	2.	5.8
M_5	10°	---	2.	9.0

Excitation of the ν_R=1 resonance via a field first harmonic is used to produce sufficient turn separation

at the deflector entry, as shown in Fig. 16. Proximity of the $\nu_R+2\nu_z=3$ resonance demands however considerable attention in choosing a not too far out extraction radius, because deterioration of the axial phase space sets in quickly. For example, for the particular field level to which Fig. 16 refers, the energy of 199 MeV/n corresponds to ν_R and ν_z values of .81 and 1.03 respectively, thus comfortably away from the resonance. The resulting axial phase space at the deflector entry is then shown by the solid line in Fig. 17. If at the same field level extraction is attempted at an energy of 199.5 MeV/n, which corresponds to a deflector entrance radius of 40.55" (i.e. .2" farther out), then the axial phase space turns to the dashed line of Fig. 17. At this radius, in fact, ν_R and ν_z are .78 and 1.1 respectively, thus very close to the resonance.

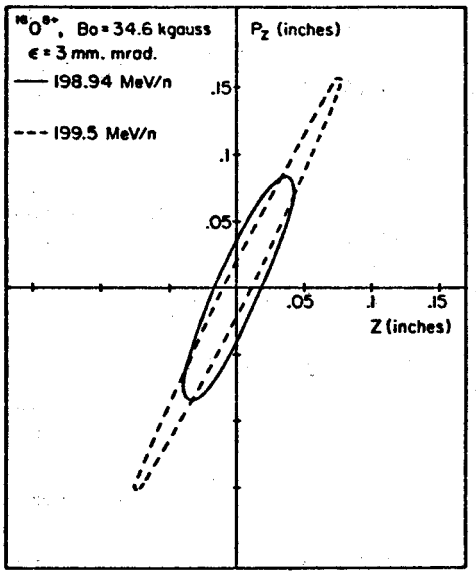

Fig. 17. Axial phase space at deflector entrance for two different particle energies. See text for details.

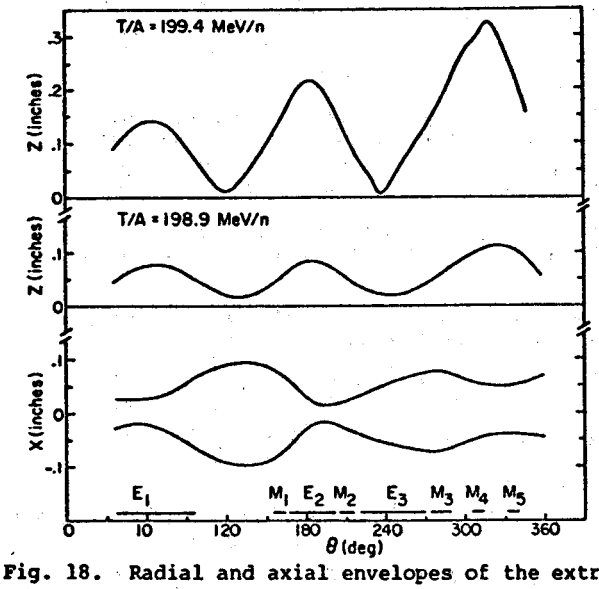

Fig. 18. Radial and axial envelopes of the extracted beam. See text for details.

Extracted beam envelopes are shown for both these cases in Fig. 18. It is seen that the beam extracted at 40.35" is extremely well confined, both radially and vertically, to within ≈.1", while the beam extracted at 40.55" would be more spread out vertically. Obviously the former solution has been chosen, since gains in somewhat lower electric fields, or faster extraction, do not really make up for the worse beam behaviour.

The present extraction scheme has been tested for other cases of particles and energies, showing that extraction is indeed always possible with, of course, reduced electric fields for less relativistic particles. Typically, electric fields of 130 kV/cm are needed for the extraction of iodine at 110 MeV/n, and 30-40 kV/cm for uranium at 20 MeV/n. At this stage it is believed that the deflectors will have to be radially movable, approximately within ≈.1", in order to allow extraction with a practically constant exit trajectory over the whole operating range. This point will need, however, a much more detailed investigation. Field perturbation produced by the magnetic channels will be compensated in a way similar to that used for the K=500 cyclotron.

Summary

A list of typical beams and operating parameters is given in Table IV as an assessment of overall machine performance.

Table IV Typical beams.

Ion	T_2/A (MeV/n)	T_1/A (MeV/n)	h_1/h_2	ν_{RF} (MHz)	Z_2/Z_1	% strip.	Bo_2 (kG)	Bo_1 (kG)
^{16}O	200	7.2	3/1	26.6	8/2	70	34.6	46.1
^{16}O	100	4.1	3/1	20.1	7/2	30	29.9	34.9
^{63}Cu	160	6.1	3/1	24.4	25/7	27.	40.0	47.6
^{63}Cu	80	3.4	3/1	18.2	23/6	27.	32.5	41.6
^{127}I	110	4.5	3/1	20.9	40/12	20.	43.3	48.1
^{127}I	70	3.0	3/1	17.2	37/10	20.	38.4	47.4
^{238}U	50	1.6	7/2	29.5	49/14	11.	46.6	46.6
^{238}U	40	1.3	7/2	26.6	44/12	15.	46.8	49.0
^{238}U	30	1.4	3/1	11.6	44/13	15.	40.8	46.1
^{238}U	20	.9	3/1	9.5	38/10	15.	38.9	49.3

In summary, this study shows that the design of a superconducting cyclotron for a range of energies and particles like the one aimed at in this project has to be pursued in great detail, just to establish an effective feasibility. In particular, an energy of 200 MeV/n for fully stripped ions looks close to the upper practical limit for a three sector machine. On the other hand, problems like extraction, isochronous field trimming, and injection can be solved without undue construction difficulties, or in other words, in a way similar to that in use for lower energy superconducting cyclotrons.

As an overall conclusion, the present results look firm enough to justify the detailed engineering study which would be needed to produce a final design of the K=800 cyclotron.

References

[1] H.G. Blosser et al., MSUCL-222A, Sept. 1976, unpublished.

[2] G. Bellomo, E. Fabrici, and F. Resmini, "Injection studies for the K=800 superconducting cyclotron at MSU," paper at this Conference.

[3] G. Bellomo and F. Resmini, "A method for minimizing trim coil power requirements in a superconducting cyclotron," paper at this Conference.

[4] H.G. Blosser, D. Johnson, and R.J. Burleigh, "Proceedings of VII Int. Conf. on Cyclotrons (Birkhauser, Basel, 1975) p. 584.

[5] M.M. Gordon, Annals of Physics 50, 571 (1968).

INJECTION STUDIES FOR THE K=800 SUPERCONDUCTING CYCLOTRON AT M.S.U.

G. Bellomo, E. Fabrici, and F. Resmini

Introduction

Beam injection from the K=500 superconducting cyclotron, now under construction at MSU, into the proposed K=800 cyclotron obviously plays a major role in the successful coupling of the two cyclotrons. Let us recall that anticipated maximum beam energies[1] are between 200 MeV/n and 50 MeV/n for fully stripped light ions and heavy ions (uranium) respectively. Minimum energies for the same extreme cases are 50 MeV/n and 5 MeV/n. Operating center field values are between 30 kG and 47 kG, and Z/A values of accelerated particles range from 0.1 to 0.5. Focusing and bending requirements lead to a 41" pole radius machine, and a three sector geometry, having 46° wide hills, with an unusually tight spiral, i.e. with a constant of 1/13 rad/inch.

Although schemes of beam injection into superconducting cyclotrons have been studied before,[2,3] they were not addressed to machines with such a wide range of beam energies and extreme sector spiral. Furthermore, they concerned injection from electrostatic accelerators, while, as will be seen in the following, coupling between two cyclotrons imposes additional constraints on the injection scheme.

Therefore, an extensive study of the injection process was carried out. This led us to consider a rather new pole tip geometry as an alternative to a conventional spiral, in order to meet all injection requirements. It is the purpose of this paper to discuss in some detail the relative merits of the two solutions presently available.

Outline of Injection Requirements and Constraints

The main requirements are:

a. If at all possible, stripping should take place in a hill, to avoid having the stripping foil positioning and replacement mechanism inside a dee.

b. Injection trajectories should have an almost constant azimuthal entry position into the cyclotron, i.e. spanning 20-40 degrees at most.

c. As a consequence of (b), all trajectories could then originate from a fixed point outside the cyclotron. If the distance of this point is conveniently chosen, typically two to three times the cyclotron radius, then steering of just a few degrees at this point will assure for every beam the proper azimuthal entry position into the cyclotron.

d. Proper phase space matching to the cyclotron acceptance, both in the radial and axial spaces, should be possible.

Let us briefly review those aspects of the coupling of the two cyclotrons which pose intrinsic constraints on beam injection. We define: h, Z, Bo, Rex, and T/A as the harmonic number, charge state, center field value, extraction radius, and extraction energy of the first cyclotron (K=500) or second cyclotron (K=800), according to the subscript.

The basic requirement in the coupling of the two cyclotrons is that the R.F. acceleration frequencies in the two machines be the same. This hypothesis leads to the following consequences:

- The second cyclotron acts just as an energy multiplier, so that in a non-relativistic approximation it must be:

$$\frac{T_2}{A} / \frac{T_1}{A} = \left(\frac{Rex_2 \cdot h_1}{Rex_1 \cdot h_2}\right)^2 \qquad (1)$$

Thus, for any given final energy per nucleon, the injection energy depends solely upon the harmonic coupling ratio (HCR).

- The stripping radius R_S in the K=800, corresponding to the injection energy T_1/A, can be expressed as

$$R_S = Rex_1 \frac{h_2}{h_1} \qquad (2)$$

and therefore, for a given Rex_1 (in our case 26.4"), it is constant for any given HCR and does not depend upon charge state or energy of the ion.

- The stripping ratio Z_2/Z_1 must obey the relationship

$$Z_2/Z_1 = \frac{h_1 \, Bo_1}{h_2 \, Bo_2} \qquad (3)$$

On the other hand, from the hard edge approximation, a limit can be derived for the lower limit of the admissible stripping ratio for injection, i.e.:

$$Z_2/Z_1 \geq \frac{1}{2}\left(\frac{Rex_2}{Rex_1}\frac{h_1}{h_2} + 1\right) \qquad (4)$$

In our case, since $\frac{Rex_2}{Rex_1} \simeq 1.5$, one obtains, for typical HCR of 3:1, 4:1, and 5:1, lower limits of $Z_2/Z_1 = 2.8, 3.6, 4.4$, respectively. Although the hard edge approximation is not really verified in a realistic cyclotron, the limits given by the above formula represent very reasonable guidelines.

Careful analysis of the operating range of the K=800 cyclotron has determined[1] that only the following harmonic coupling ratios are possible:

- 3:1, 4:1, 5:1 for beam energies between 200 MeV/n and 18 MeV/n, the lower limit being imposed by the R.F. frequency. Corresponding average stripping radii are 8.8", 6.6", and 5.2".

- 5:2 and 7:2 for energies between 5 MeV/n and 60 MeV/n, in this case the upper limit being determined again by the R.F. frequency. Corresponding stripping radii are 10.5" and 7.5".

In view of the above constraints, the self-consistent analysis of beam injection involves the following steps:

- Determine the ranges of stripping ratios needed for each harmonic coupling, over the whole $(Bo_2, Z_2/A)$ operating range. These must satisfy the relationships (2), (3), and (4) and the Z_2 values must also, for each energy, be at,or around,the peak for maximum intensity at stripping.[1]
- Determine an injection scheme which fulfills requirements (a), (b), and (c) set forth above.
- Determine the real lower and upper limits of the stripping ratio Z_2/Z_1 which are compatible with the selected injection scheme. This must be done for each of the five possible harmonic couplings over the entire range of Bo_2, Z_2/A.
- Verify that the Z_2/Z_1 limits thus derived allow the desired coupling of the two cyclotrons.

- Examine the phase space behaviour of the injected beams and establish the proper matching conditions.

Possible Injection Schemes

Injection both against and along the spiral has been considered. As expected, the former restricts severely the range of allowed stripping ratios and therefore injection along the spiral, and more precisely in a valley, was selected.

The resulting scheme is shown in Fig. 1, where most cases of light ions for a final energy of 200 MeV/n are presented, encompassing HCR of 3:1, 4:1, and 5:1. The latter two modes are needed for boron and carbon injection respectively, with corresponding stripping ratios of 5 and 6, which cannot be injected in the 3:1 mode. All trajectories, tracked up to the radius of 52", converge to a common point, not shown in the figure, which lies 150" from the cyclotron center[1] at an azimuth of 60°. Decreasing stripping ratios correspond to trajectories of progressively lower average curvature radius, as would be expected also in a hard edge approximation, being:

$$\rho_{inj} = R_S \frac{z_2}{z_1} \qquad (5)$$

The main difficulty with this scheme is that stripping occurs naturally in a valley. This is mostly a geometrical effect, arising from the tight spiral of the sectors, and it can be predicted also on the basis of the hard-edge approximation. Displacing the trajectories to a hill, although possible in principle, is not practical because the increased average magnetic field along the trajectory restricts the allowable stripping ratios range.

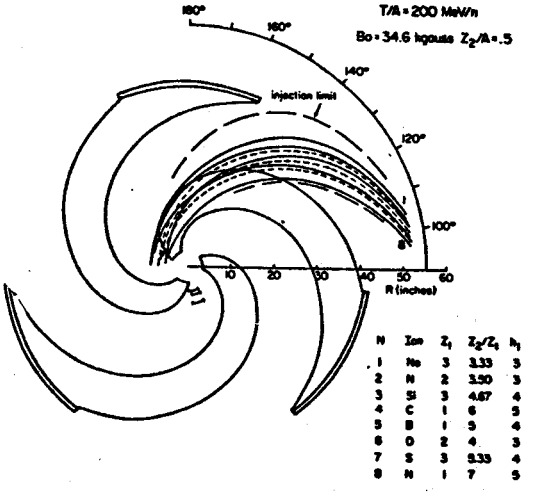

Fig. 1. Injection trajectories for 200 MeV/n light ions (conventional spiral, 1/13 rad/inch constant).

We designed therefore a different sector geometry, in which the spiral constant is positive, with the same 1/13" constant, up to a radius of 15" and it reverts to a negative constant thereafter. This scheme, shown in Fig. 2, produces the effect of substituting hills to valleys in the useful range of stripping radii (up to 12") with a narrow, 2" in radius, transition region between the two spirals.

Injection trajectories are also shown in Fig. 2, again for 200 MeV/n final energies. Now stripping for all particles effectively occurs in a hill, all other characteristics of injection remaining equal.

The only drawback of such a double spiral geometry is the decrease of vertical focusing, which can be expected in a radial region of 3"-4" around the transition radius of 15", the sectors being there practically radial.

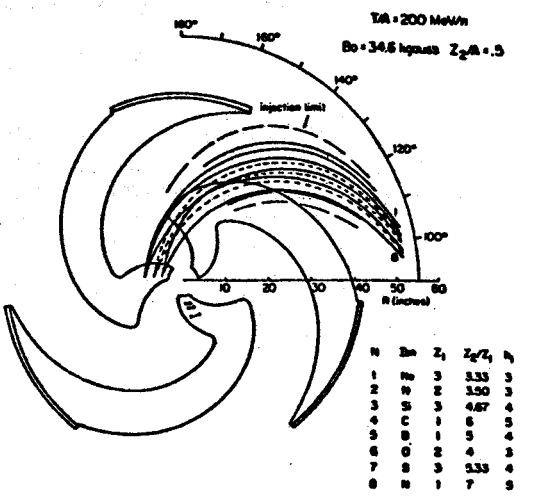

Fig. 2. Injection trajectories for 200 MeV/n light ions (double spiral scheme).

Equilibrium orbit data show, however, that the transition region presents no danger of beam losses. Vertical focusing frequencies for 200 MeV/n and 20 MeV/n particles are shown in Fig. 3, both for the conventional and double spiral geometry. Since the minimum ν_z values are about .1 and .14 respectively, we concluded that the double spiral scheme is a realistic alternative for injection in the K=800 machine.

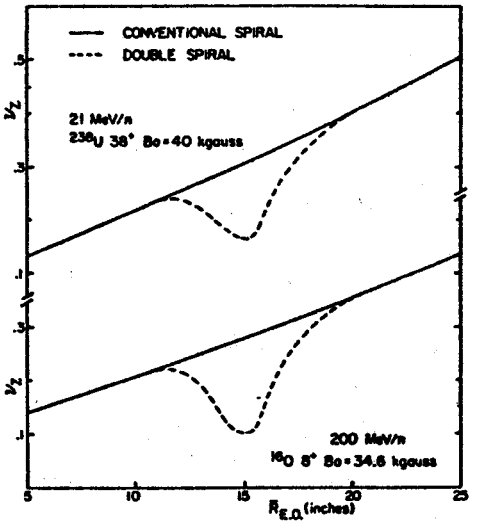

Fig. 3. Axial focusing frequencies, ν_z for the conventional spiral and the double spiral scheme.

Detailed Analysis of the Injection Solution

The ranges of stripping ratios compatible with the proposed scheme have been studied in great detail. For each h_1/h_2 ratio, minimum and maximum values of the allowed stripping ratio will exist, as shown by the trajectories indicated as injection limits in Fig. 2. In particular the maximum z_2/z_1 value usually corresponds to the hill azimuthal limit at the proper stripping radius. The minimum is more often associated with the intrinsic limit on the radius of curvature of the injection trajectory, like the one given by eq. (5).

The actual limits of the stripping ratios are of course a function of the center field level, Bo_2, and z_2/A, as can be expected because of the very different isochronous field shapes and hence the different

average field experienced by the injected particles. An example is shown for the case of $h_2:h_1=3:1$ in Fig. 4, where maximum (solid lines) and minimum (dashed lines) values of Z_2/Z_1 are plotted as a function of Z_2/A for different field levels. Marked variations are indeed observed, especially for the minimum Z_2/Z_1 values. Such an analysis has been carried out for all other harmonic coupling modes, thus giving a very comprehensive picture of the injection solution.

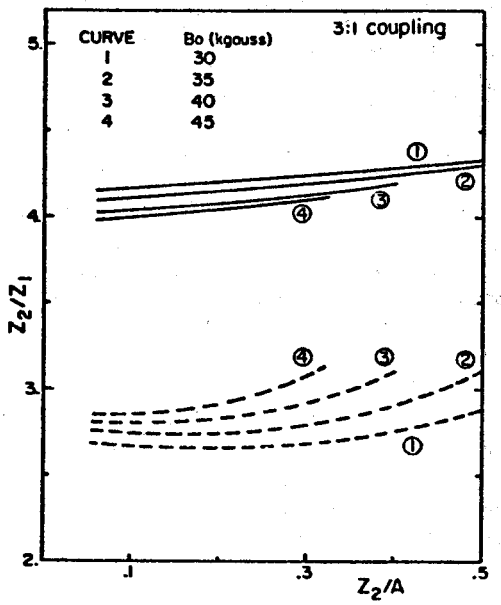

Fig. 4. Maximum and minimum stripping ratios allowed for injection, as a function of Z_2/A, for different field levels.

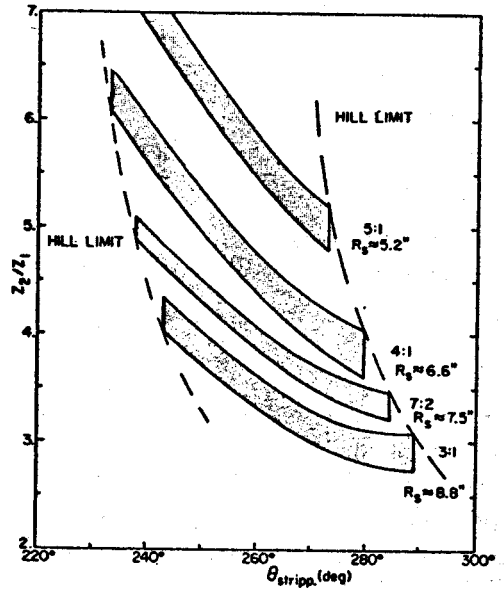

Fig. 5. Allowed stripping ratios, as a function of the stripping angle, for different harmonic couplings.

The overall results are shown in Figs. 5 and 6, where the stripping ratios compatible with the injection scheme are plotted as a function of $\theta_{stripping}$ and θ_{entry} at 40", respectively. The latter radius has been chosen because, as apparent from Fig. 2, the bundle of injection trajectories reaches there the maximum width. Fig. 5 shows that, for any given HCR, the allowed stripping ratios lie within a band. The latter is defined by:

a. The hill width limits, which are functions of the stripping radius.

b. Two curves which are roughly defined, at each stripping angle θ_s, by the maximum and minimum ion energy compatible with the given harmonic coupling. Therefore, upper limits of the 3:1, 4:1, and 5:1 bands are defined by the 200 MeV/n energy limit at B_o=34.6 kG and Z_2/A=.5. Likewise, the lower limits belong to 20 MeV/n cases. All other intermediate cases lie essentially within the band.

The same considerations apply to Fig. 6.

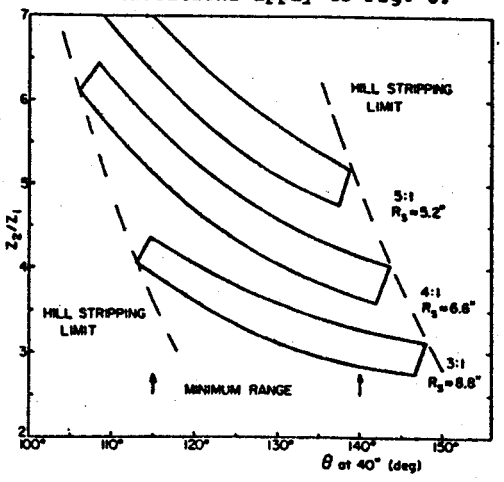

Fig. 6. Stripping ratios as a function of the entry azimuth at 40" radius, for different harmonic couplings.

As a result of this analysis we have been able to define a minimum range of entry azimuths at the radius of 40", as indicated in Fig. 6, which still allows coupling of the two cyclotrons for all required particles and energies. This minimum range corresponds to the dashed region of Fig. 2 and implies in turn a restricted range of stripping azimuths.

The injection solution thus emerging is characterized by a maximum angular width at 40" of about 25°. The corresponding azimuthal range of stripping azimuths is about 26°, i.e. considerably less than the hill width of 46°. All injection trajectories converge to a point 150" away from the cyclotron center, where a steering of ±1.5° will be sufficient to properly match all injection paths.

Phase Space Behaviour

Examples of radial and axial phase space behaviour of typical beams along the injection trajectory are shown in a self-explanatory way in Figs. 7 and 8. The calculations were made on the assumption of matching the accelerated beam eigenellipses of 6 mm·mrad emittance at the stripping radius. As expected, radial defocusing of the beam is produced by the cyclotron fringing field, thus requiring a radially focused beam at the entry point at 52" radius, while practically an axial waist is needed at the same point.

The same pattern of Figs. 7 and 8 is maintained throughout the operating range of fields and stripping ratios. A marked correlation showed up, however, between the extent of radial defocusing and the position of the injection trajectory with respect to the sectors. This is illustrated in Fig. 9, where the maximum x and p_x values at 52" radius, thus corresponding to the extreme points of the radial phase space figure, are plotted as a function of the stripping ratio. Since the case presented here refers to the trajectories of Fig. 2, it is easy to appreciate that the maximum defocusing occurs for those trajectories

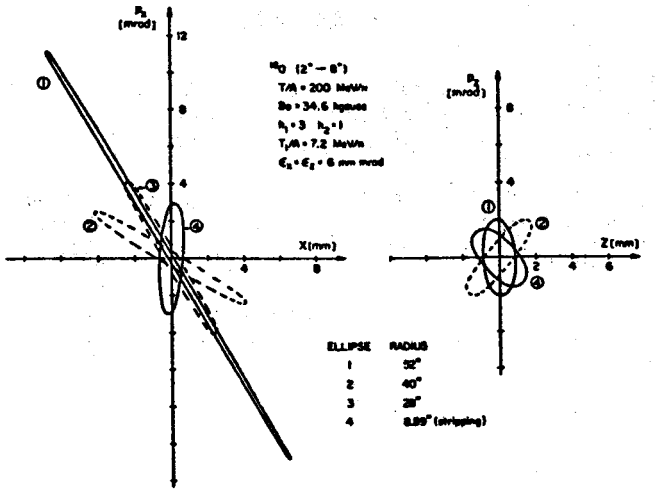

Fig. 7. Radial and axial phase space of an injected oxygen beam for a final energy of 200 MeV/n.

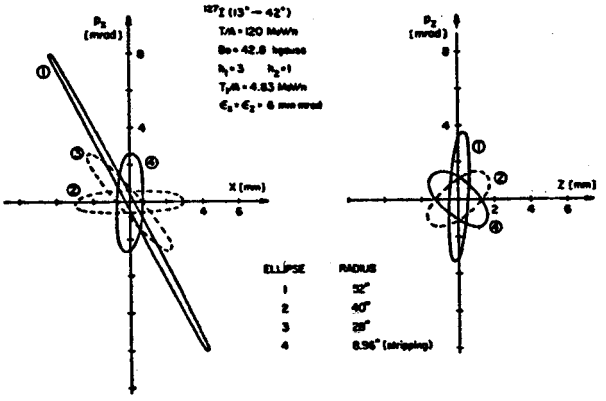

Fig. 8. Radial and axial phase space of an injected iodine beam for a final energy of 120 MeV/n.

which coast along the hill-valley boundary, thus experiencing a stronger, radially defocusing field gradient. The effect is even stronger in the case of a conventional spiral (dashed lines of Fig. 9) as examination of the trajectories of Fig. 1 would also lead to expect.

The corresponding analysis of the (z,p_z) phase space is presented for the same cases in Fig. 10. The relative behaviour of (z,p_z) for the double spiral reflects a constant axial waist situation at 52", as anticipated above.

In the conventional spiral, the counterpart of a large radial defocusing is instead a sharp axial focusing. Comparison of the radial and axial phase space pattern suggests therefore that the double spiral scheme should be preferred.

Since the effect on phase space is clearly dependent only upon the geometry of the injection trajectory relative to the sectors, and since the latter span the same space region for all harmonic coupling modes, one should expect two consequences:

- The same behaviour should be present for all HCR.
- The radial defocusing effect should be stronger the lower the field, since the local defocusing field index, as seen by the particles along the sector, is only dependent upon the field level.

Both these conclusions are supported by a number of calculations. This can be seen in a self-explanatory way in Fig. 11 for the first point and Fig. 12 for the second.

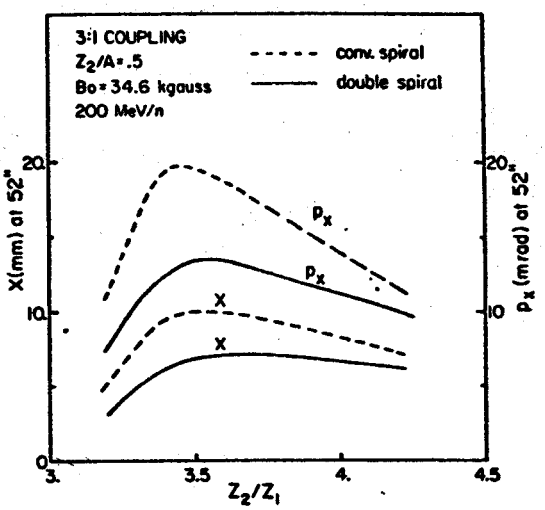

Fig. 9. Maximum (x,p_x) values at 52" radius for injected beams of 6 mm·mrad emittance (see text for details).

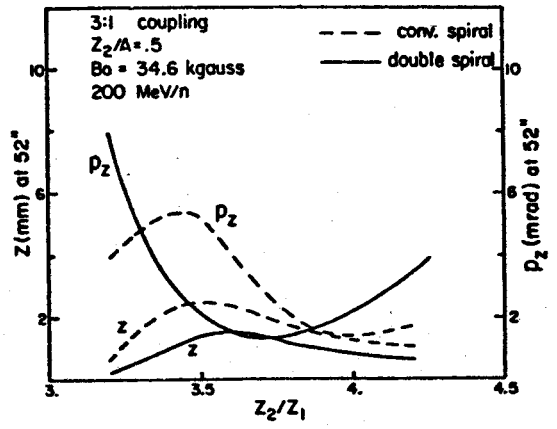

Fig. 10. Maximum (z,p_z) values at 52" radius for injected beams of 6 mm·mrad emittance (see text for details).

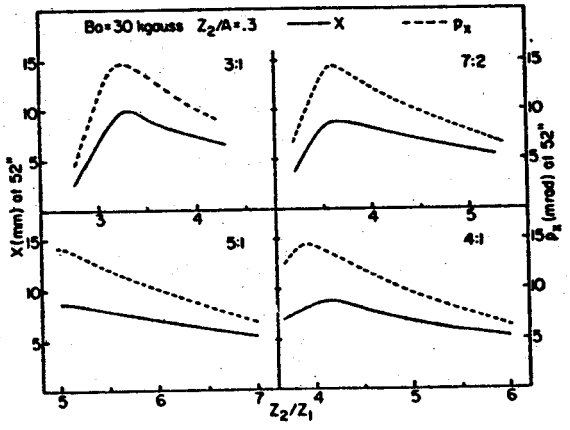

Fig. 11. Maximum (x,p_x) values at 52" radius for different HCR as a function of the stripping ratio (6 mm·mrad emittance).

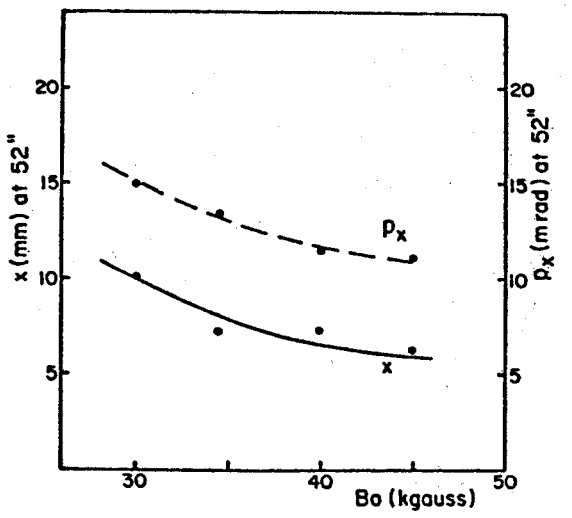

Fig. 12. Absolute maximum values of x and p_x at 52" radius as a function of the field level for a 6 mm·mrad emittance.

Conclusions

The analysis carried out so far indicates that the double spiral scheme has two main advantages over a conventional spiral:

- Hill stripping is possible for all harmonic coupling modes and all stripping ratios necessary for the proper coupling of the two cyclotrons.
- It presents a better phase space behaviour.

Admittedly, this scheme also has the disadvantage of a limited decrease in vertical focussing, albeit restricted to a narrow radial region, and of a somewhat more complex mechanical design for the pole tip. In our view, however, these should be considered as minor problems when compared to the advantages outlined above.

Phase space studies show that no extra focusing channel is needed inside either the yoke or the cryostat. In fact, if the matching quadrupoles can be positioned close enough to the cyclotron yoke, say 20" to 40", the results of phase space tracking indicate that quadrupole apertures of 4" are adequate for matching the required radial and axial beam shapes. This would of course involve a displacement of the quadrupoles, together with the central ray injection trajectory. This displacement being, however, limited to a few degrees, it should certainly be preferred to a movable focusing element inside the cyclotron.

No second order calculations have been carried out so far. This refers mostly to matching in the (E,t) subspace, where other effects may be present. Transit time spreads from the entry point at 52" to the stripping radius have, however, been computed for all beams investigated in this analysis. Maximum spreads between 2° and 3° were found which should constitute no real problem for the cyclotron coupling.

Although more detailed calculations will undoubtedly be needed on these aspects of injection, the presently envisaged scheme seems to constitute a very realistic and practical one.

References

[1] F. Resmini, G. Bellomo, E. Fabrici, H.G. Blosser, and D.A. Johnson, "Design characteristics of the K=800 superconducting cyclotron at MSU," paper at this Conference.

[2] J.H. Ormrod et al., "Status of the Chalk River superconducting heavy ion cyclotron," Proceedings of the 1977 Particle Accelerator Conference, IEEE NS-24, (1977) 1093.

[3] E. Acerbi, G. Bellomo, C. de Martinis, and F. Resmini, "Injection studies for the proposed superconducting cyclotron at the University of Milan," Proceedings of the 1977 Particle Accelerator Conference, IEEE NS-24, (1977) 1112.

A METHOD FOR MINIMIZING TRIM COIL POWER REQUIREMENTS IN SUPERCONDUCTING CYCLOTRONS*

G. Bellomo and F. Resmini

Introduction

A key issue in the design of superconducting cyclotrons is to obtain a properly isochronous field over the wide range of particles and energies usually demanded. In this respect it is useful to recall that in superconducting cyclotrons the main coils produce a large fraction of the total average field, and that the field produced by the saturated iron is very nearly constant over the 20-50 kG range usually employed.

The main problem is therefore to optimize the main coil design, and to optimize the field generated by the iron, in order to minimize the total power requirements for trim coils. Detailed studies for the proposed K=800 machine at MSU, which requires isochronous fields for ion energies spanning from 5 to 200 MeV/n, led us to develop a method which effectively helps in solving the problem. In the process, we found some results which seem to have an overall validity and therefore have some implications for superconducting cyclotron design. It is the purpose of this paper to review in some detail the procedure used and the main consequences pertaining to the K=800 design study.

Outline of the Method

We assume the main coils to be split into two vertical sections, subscripts α and β referring to the lower section (closer to the median plane) and upper one. The following notation will be used throughout:

- $F_\alpha(r)$, $F_\beta(r)$, $F_k(r)$ = form factors of the main coil sections and of the kth trim coil (with resistance R_k, N coils total).
- I_α, I_β, I_k = corresponding currents
- $B_{iron}(r)$, $B_{is}(r)$ = magnetic field generated by the iron configuration and isochronous field required by a given ion
- $\epsilon(r)$ = field error, with respect to isochronism.

We shall then write, for any ion:

$$B_{is}(r) = B_{iron}(r) + F_\alpha(r)I_\alpha + F_\beta(r)I_\beta + \sum_{K=1}^{N} F_k(r)I_K + \epsilon(r) \qquad (1)$$

It is obvious that given $B_{iron}(r)$, $F_\alpha(r)$, $F_\beta(r)$, and $F_k(r)$, ordinary least squares fitting will yield the I_α, I_β, and I_k values which minimize $\sum_r \epsilon^2(r)$.

It is also obvious that for any particular ion, and whatever the functions $F_\alpha(r)$ and $F_\beta(r)$ are, there will always be a function $B_{iron}(r)$ for which the currents I_k and the errors $\epsilon(r)$ in that particular case equal zero.

The problem to which we address ourselves can instead be schematized as follows:

- Given a main coil, i.e. $F_\alpha(r)$ and $F_\beta(r)$, and trim coil form factors $F_k(r)$, determine, if it exists, a $B_{iron}(r)$ which minimizes:

  $\Sigma\, \epsilon^2(r)$ and $P = \sum_{K=1}^{N} R_k I_k^2$ (total trim coil power)

  over the desired range of ions and energies.
- As a consequence, optimize the main coil design, with the aim to minimize the total trim coil power.

Our method is based upon the selection of two appropriate particles which, for the present purpose, can be thought of as representative of the extreme isochronous fields required, like the least and most relativistic particles in the operating range of the cyclotron.

If we write eq. (1) for these two ions, represented by subscripts 1 and 2 on the relevant quantities, and then subtract the two equations, we get:

$$[B_{1is}(r) - B_{2is}(r)] = [B_{1iron}(r) - B_{2iron}(r)] + F_\alpha(r)[I_{1\alpha} - I_{2\alpha}] + F_\beta(r)[I_{1\beta} - I_{2\beta}] + \sum_{K=1}^{N} F_k(r)[I_{1k} - I_{2k}] + [\epsilon_1(r) - \epsilon_2(r)] \qquad (2)$$

with self-explanatory notation.

Let us now make the simplifying hypothesis:

$$B_{1iron}(r) - B_{2iron}(r) \equiv 0 \qquad (3)$$

for every radius.

This physically corresponds to an invariable field produced by the saturated iron configuration. Although not exactly fulfilled in reality, it nevertheless is an accurate enough hypothesis for the present purposes. We shall anyhow examine later the consequences of it not being strictly verified.

Equation (2) can then be written as

$$\Delta B_{is}(r) = F_\alpha(r)\Delta I_\alpha + F_\beta(r)\Delta I_\beta + \sum_{K=1}^{N} F_k(r)\Delta I_k + \Delta\epsilon(r) \qquad (4)$$

where the symbol Δ represents the differences in eq. (2).

Having eliminated $B_{iron}(r)$, equation (4) lends itself to a minimization, with an ordinary least squares fitting procedure, of the quantitity: $\sum_r [\Delta\epsilon(r)]^2$, thus obtaining values of:

$$\Delta I_\alpha = I_{1\alpha} - I_{2\alpha} \qquad (4a)$$
$$\Delta I_\beta = I_{1\beta} - I_{2\beta}$$
$$\Delta I_k = I_{1k} - I_{2k}$$

One can prove[1] that if $\sum_r [\Delta\epsilon(r)]^2$ is minimized with a least squares fitting, then also

$$\sum_r \epsilon_1(r)^2 + \sum_r \epsilon_2(r)^2 \quad \text{and} \quad P_1 + P_2$$

will be minimized, if

- $\epsilon_1(r) + \epsilon_2(r) = 0$ for every radius (5)
- $I_{1k} + I_{2k} = 0$ for every trim coil

This finding has the following consequences:

- Given two ions, and for given main coils and trim coils, there exists an absolute minimum of the trim coil power needed for providing an isochronous field in the two cases. This minimum value is obtained by least squares fitting of eq. (4), imposing thereafter condition (5). This power is thus equal for both ions, and corresponds to equal and opposite currents for each trim coil.
- To reach the condition of absolute minimum power the pole tips must produce a $B_{iron}(r)$ which satisfies for every radius the following equation:

*This material is based upon work supported by the National Science Foundation under Grant No. Phy 78-01684.

$$B_{1is}(r) + B_{2is}(r) = 2\,B_{iron}(r) + F_\alpha(r)[I_{1\alpha} + I_{2\alpha}] + F_\beta(r)[I_{1\beta} + I_{2\beta}] \quad (6)$$

where:

- the terms of eq. (1) have been summed, rather than subtracted, for the two ions
- $B_{iron}(r) = B_{1iron}(r) = B_{2iron}(r)$ according to (3)
- the errors $\varepsilon(r)$ and the trim coil currents I_k cancel out according to (5)

In eq. (6) there are four unknowns, namely $I_{1\alpha}$, $I_{2\alpha}$, $I_{1\beta}$, and $I_{2\beta}$, while, according to (4a), ΔI_α and ΔI_β are known via least squares fitting. As a consequence, there are ∞^2 $B_{iron}(r)$ functions which yield an absolute minimum for trim coil powers. However, if one specifies in eq. (6) the $B_{iron}(r)$ values at two conveniently chosen radii R_1 and R_2, one has a set of four linear equations, which will yield $I_{1\alpha}$, $I_{1\beta}$, $I_{2\alpha}$, and $I_{2\beta}$. Henceforth the values at all radii of the ideal $B_{iron}(r)$, which assumes at R_1 and R_2 the specified values, can be calculated through eq. (6).

It will also be recognized that whatever values of $B_{iron}(r)$ are chosen at R_1 and R_2, and whatever the radii R_1 and R_2, this will only affect the partial currents I_α and I_β and not the trim coil power required for either case.

Given the "ideal" $B_{iron}(r)$ function thus calculated, and which shall henceforth be denoted by $B_{best}(r)$, one can readily calculate the trim coil powers needed for any other ion, by least squares fitting through eq. (1). One should further note that the resulting trim coil power, the trim coil contributions, and the field errors will in any case be independent[1] of the particular $B_{best}(r)$ function chosen.

In summary, the method entails the following steps:

1. Choose two ions which represent extremes in field isochronism requirements.
2. Carry out the least squares fitting over all radii, according to (4), and determine the minimum power required using condition (5).
3. Determine a convenient $B_{best}(r)$ function. In this respect, it is obvious that radii R_1 and R_2 shall typically be chosen close to the innermost and outermost radii of the cyclotron.
4. Map the trim coil power requirements for all other ions.

At this point we note that if a generic $B_{iron}(r)$ function is chosen, instead of the $B_{best}(r)$ determined by the above procedure, the following consequences will arise for the two representative ions:

- The sum of the powers, P_1 and P_2 (which will not be equal anymore) will increase by the amount
  $\Delta P = 2\sum_k R_k(\Delta I'_k)^2$
- The sum of the errors, $\sum_r \varepsilon_1^2(r)$ and $\sum_r \varepsilon_2^2(r)$, will increase by
  $\Delta\varepsilon = 2\sum_r(\Delta\varepsilon'(r))^2$
  where $\Delta I'_k$ and $\Delta\varepsilon'(r)$ are given by a least squares fitting at all radii of:

$$\Delta B_{iron}(r) = F_\alpha \Delta I'_\alpha + F_\beta \Delta I'_\beta + \Sigma_k F_k \Delta I'_k + \Delta\varepsilon'(r) \quad (7)$$

$\Delta B_{iron}(r)$ representing the error: $B_{best}(r) - B_{iron}(r)$.

Results for the K=800 Design

The following two ions have been chosen as extremes:

- A fully stripped light ion, Z/A=.5, with center field of 34.6 kG, corresponding to a final energy of 200 MeV/n.
- A uranium ion, charge state 38^+, Z/A=.16, center field of 40 kG, corresponding to 20 MeV/n. This is the least relativistic particle, at the maximum field, which can be accelerated in 1st harmonic, the latter mode covering about 80% of the machine operating range.

Although final results suggest that different choices may be more appropriate, nevertheless this is a very realistic starting point. Isochronous fields are computed on the basis of the field modulation produced by the sectors. Fits, as required by eqs. (1) and (4), are made in .5" radial steps at all radii between 4" and 39.5". The latter value, which should be viewed against a pole radius of 41",[2] is then the last radius at which perfect isochronism is required, and has been chosen after a careful analysis. Comparison of fits with different final radii, from 38" to 40.5", indicated that 39.5" would be the upper limit compatible with: i) realistic phase behaviour in the fringing region, ii) fringing field generated by iron and coils for extraction at approximately 40.4". All the trends reported here retain however their validity over the range of ultimate fitting radii quoted above.

Twenty-two trim coils are used for the K=800, as described in Ref. 2. Main coils are spaced by 3" around the median plane and a maximum current density of 3500 A/cm^2 is allowed. Coil inner radius is 45.5" with radial width of 6". As stated above, each coil is split into two sections, α and β, and we shall use the following notation:

$h_\alpha + h_\beta = H$ coil height

$h_\alpha/H = F$ partition fraction, referred to the section closer to the median plane. The two sections are separated by 0.5" axially.

The minimum trim coil power required for either representative ion, and derived from the fits according to eq. 4, is plotted in Fig. 1 as a function of the coil height and for four different partitions F. Variation of the coil radial width by 1" around 6" produces the same results. This is physically intuitive since the coils form factors, F_α and F_β, do not change appreciably, the height to width ratio being rather large for all cases. The curves of Fig. 1 point out that:

- For the same coil height, i.e. constant ampereturns, the larger the partition F, the lower is the power.
- For the same partition the power decreases by increasing the coil height.

What this means in terms of actual coil operation can be readily seen if, according to eq. 5-6 and the procedure outlined above, actual $B_{iron}(r)$ values are introduced thus obtaining the currents I_α, I_β for either ion. Values of 19.27 kG and 16.12 kG were chosen for the radii of 10" and 38", as computed for the iron configuration. This allows us to construct a diagram like the one shown in Fig. 2 for the 200 MeV/n ion. The current density needed in the upper coil, J_β, is plotted as a function of the coil height, and for

the same four partitions F. Corresponding J_α values can be read off the scale on the right. Also shown are lines of constant trim coil powers.

Several features emerge from Fig. 2, namely:

- For the same coil height, the decrease of the trim coil power for increasing partition fractions F is obtained by running the upper coil to progressively lower currents, and ultimately reversing the sign. Clearly, F values larger than 0.6 are not practical because one would rapidly approach the J_β=-3500 A/cm^2 limit.
- Reduction of the power along an F=constant line, accomplished by increasing the coil height, means also progressively larger negative values of J_β, and lower J_α.
- Optimal coil design implies therefore a compromise between: i) minimum trim coil power desired, ii) practical limit on how large a negative current can be tolerated in the upper coil because of stresses, etc., and iii) cost of progressively larger main coils.

For the K=800, we choose a total height of 26.5" and a partition fraction of .6, thus leading to minimum negative J_β≃-1000 A/cm^2 and power requirements of about 36 kW for the two extreme ions.

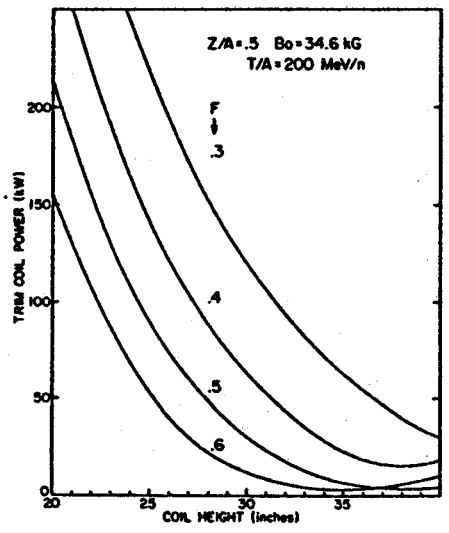

Fig. 1. Minimum trim coil power for 200 MeV/n.

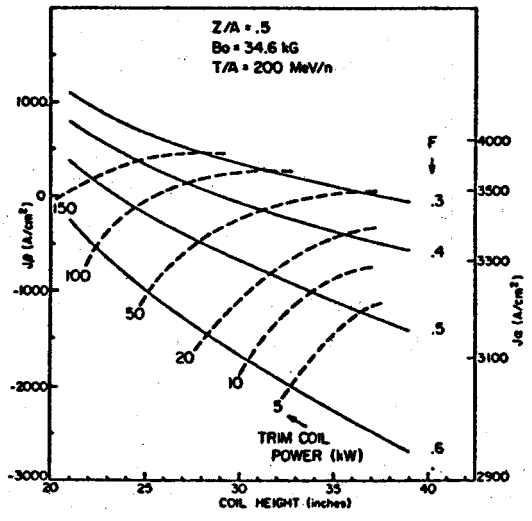

Fig. 2. Current density needed in the main coils, as a function of coil height, for 200 MeV/n.

Mapping of the powers throughout the operating range is done, as explained above, by ordinary least squares fitting once the function $B_{best}(r)$ is calculated. For these coils, and on the basis of the two ions chosen, this field is presented in Fig. 3 and compared with the actual field produced by the iron configuration. The most interesting feature is the increase of about 180 Gauss required for the ideal field around the radii 39"-40". Calculations with local corrections of the hill profile show that there is no problem in matching the desired field. We also recall that, according to eq. (7), failure to provide the required field shape would enhance the power from 36 kW to about 80 kW for the 200 MeV/n ion.

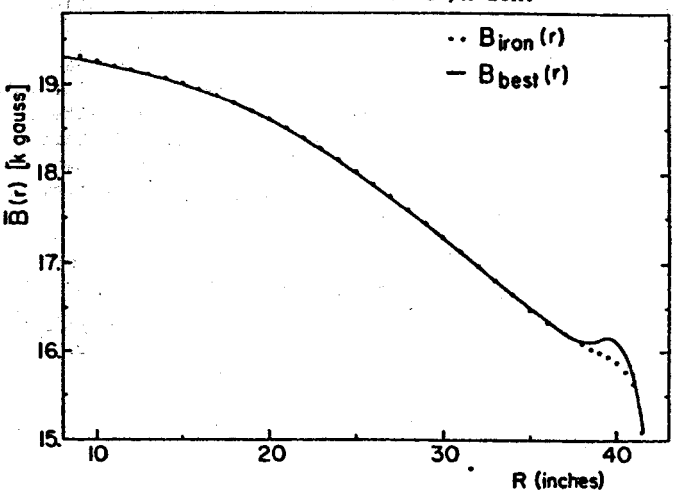

Fig. 3. $B_{best}(r)$ and $B_{iron}(r)$ (see text for details).

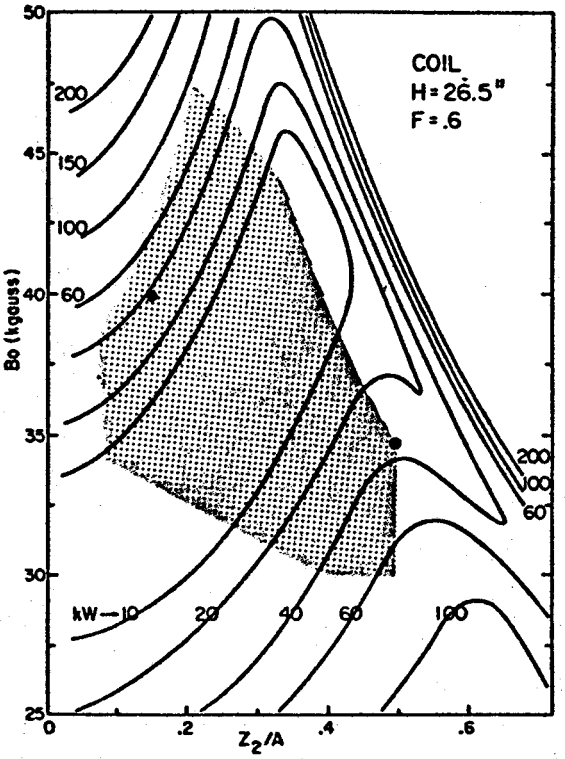

Fig. 4. Trim coil power contours for the K=800 operating range. Coil height=26.5", partition F=.6

Contours of constant trim coil power obtained by using the calculated $B_{best}(r)$ are presented in Fig. 4, in the (Bo, Z/A) plane, with reference to the operating diagram of the machine.[2] This is also done for comparison for two other coils, namely a coil of the same height but partition fraction equal to 0.4, Fig. 5,

and a coil of larger height, 30", and the same partition of .6, in Fig. 6. The positions of these coils on the diagrams of Figs. 1 and 2 can be easily recognized. Needless to say, the $B_{best}(r)$ function for each coil is slightly different, although it still assumes the values of 19.27 and 16.12 kG at 10" and 38" radius respectively, and is calculated on the basis of the same two representative ions. All the fits reported here turned out to be of remarkable quality, with departures from the ideal isochronous field confined to a few Gauss at most. This is obviously to be ascribed to the use of a theoretical $B_{best}(r)$, and therefore shows the importance of approximating the above function as closely as possible in the real field.

Comparison of the three figures shows that the power requirements for the different coils follow throughout the operating region the same pattern apparent from Figs. 1 and 2, and therefore that the procedure established on the basis of just two representative ions allows a meaningful optimization of the main coil design.

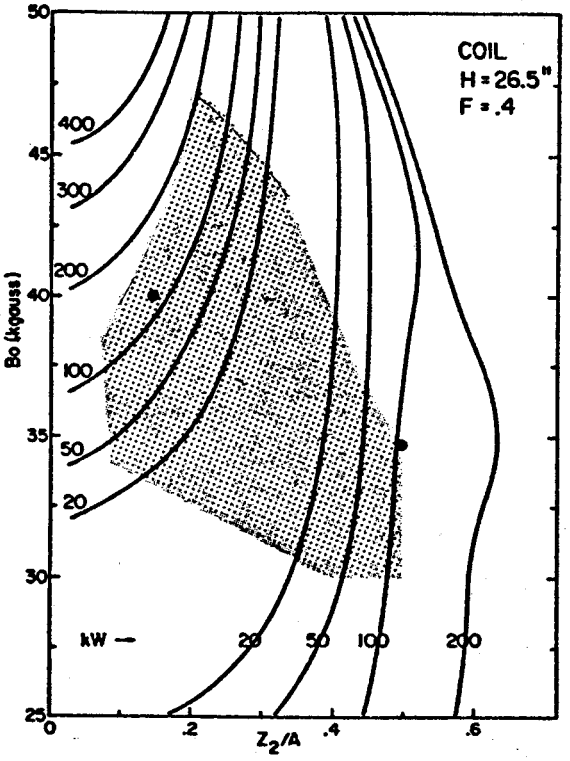

Fig. 5. Trim coil powers contours for the K=800 operating range: Coil height =26.5", partition F=.4.

For a closer analysis of the cases pertaining to our optimized coil design, the contours of constant current densities J_α and J_β are shown, again in the (Bo, Z/A) plane, in Fig. 7. The margins with respect to the 3500 A/cm^2 limit and the need to have J_β negative over a part of the operating range can be appreciated.

Typical field corrections given by the trim coils are presented in Fig. 8, both for the two representative ions and for other cases corresponding to lower and higher powers according to the coils and diagrams of Fig. 4. As anticipated, the field corrections have opposite signs and the behaviour as a function of radius is very much the same, different power levels being mostly characterized by different amplitudes of the field correction.

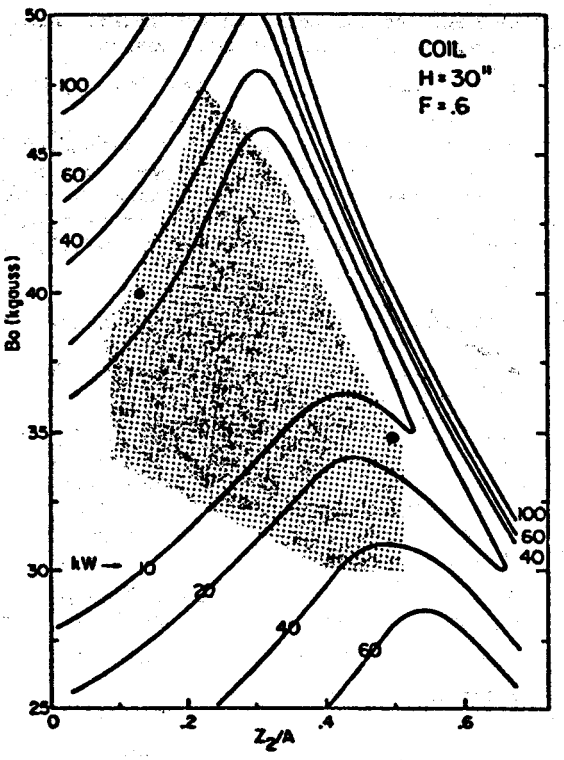

Fig. 6. Trim coil power contours for the K=800 operating range. Coil height=30", partition F=.6.

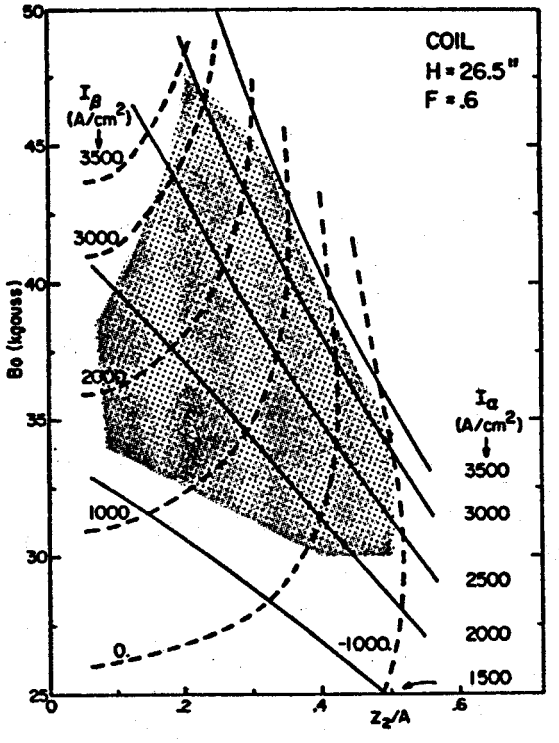

Fig. 7. Constant J_α and J_β contours for the K=800 operating range. Coil height=26.5", partition F=.6.

Trim coil currents for the three cases at the top of Fig. 8 are listed in Table I. A very smooth behaviour of the currents is observed, both in value and sign. Opposite signs hold, of course, for the cases at the bottom of Fig. 8.

Table I. Trim coil currents.

T. Coil No.	R_k (Ω)	I_k (A) $\Sigma P_k \simeq 10$ kW	$\Sigma P_k \simeq 36$ kW	$\Sigma P_k \simeq 55$ kW
1	.026	-27	-85.	-89
2	.031	-42	-127	-135
3	.035	-54	-161	-173
4	.039	-66	-191	-207
5	.043	-76	-216	-235
6	.047	-84	-234	-259
7	.051	-94	-246	-281
8	.056	-97	-250	-285
9	.060	-96	-246	-278
10	.064	-94	-234	-267
11	.068	-90	-213	-247
12	.072	-83	-185	-219
13	.076	-73	-150	-183
14	.080	-61	-108	-139
15	.085	-45	-61	-89
16	.089	-25	-12	-33
17	.093	-2	+37	+27
18	.097	+26	+82	+86
19	.101	+55	+115	+139
20	.105	+87	+133	+181
21	.109	+111	+120	+192
22	.114	+151	+93	+202

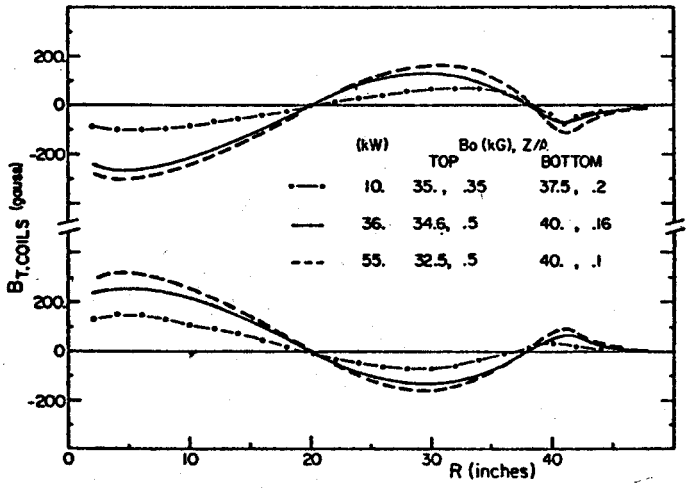

Fig. 8. Trim coil field contributions for different power levels and ions.

The peculiar behaviour of the equipower contours suggests that:

- The representative ions for defining the power limits should really be the ion with maximum Z/A at the minimum field, and that with minimum Z/A at the maximum field.
- Different choices might lead to very misleading results, or in other words to an equipower contour diagram not properly centered over the machine operating range.

As an example, Fig. 9 presents the contours which would be obtained should one choose as representative ions the same most relativistic particle (200 MeV/n, Z/A=.5, Bo=34.6 kG) and the least relativistic particle at the minimum field, i.e. 4 MeV/n, Z/A=.08, Bo=34 kG. It is quite evident that with respect to the overall operating diagram there is a definite unbalance of the required trim coil powers.

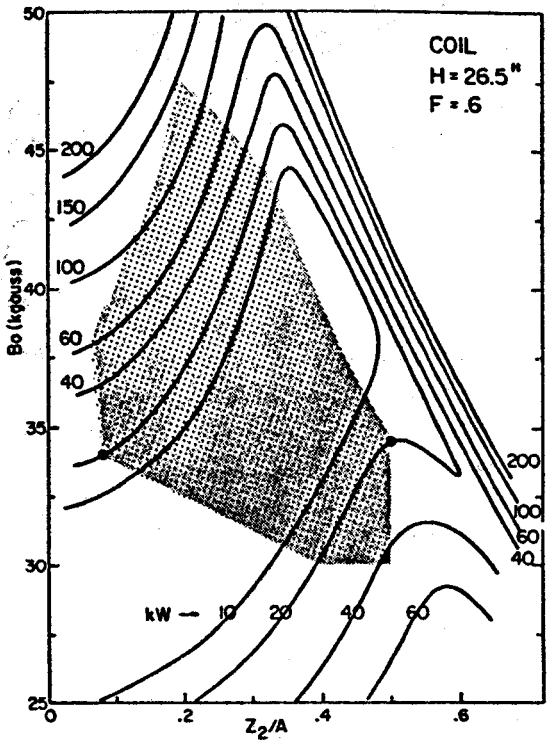

Fig. 9. Trim coil power contours for coil height = 26.5", F=.6. The two new representative ions chosen are marked on the figure.

Further Considerations

All calculations reported here are consistent with the hypothesis of a function $B_{best}(r)=B_{iron}(r)$ independent of the field level. It is therefore appropriate to ask which variations can be expected in reality, when the $B_{iron}(r)$ will vary both in level and shape depending upon coil excitation.

So far we have carried out only a limited number of calculations. In Fig. 10 we present the iron fields which are expected at various coil excitations. Curve (1) corresponds to the B_{best} used so far (see Fig. 3) and therefore to the coil excitation needed for Z/A=.5, Bo=34.6 kG. Curve (2) shows the expected B_{iron} field for the coil excitation needed for the other representative ion, i.e. U^{38+} at Bo=40 kG.

The field differences between curves (2) and (1) are then plotted in Fig. 11, curve (a). Fit for the uranium ion in the sense of Eq. (1), using the B_{iron} of curve (2), yields a lower trim coil power i.e 22 kW instead of the original 36 kW. This is reflected in a smaller field contribution of the trim coils, curve (d) in Fig. 11, with respect to the original one, curve (c). Analysis of this unexpected result shows that, due to the level variation between the two iron fields, there is also a difference in the field produced by the main coils as shown in curve (b) Fig. 11. Since the difference between curves (a) and (b) has the same behaviour as the field correction produced by the trim coils, the consequence is the observed reduction in power.

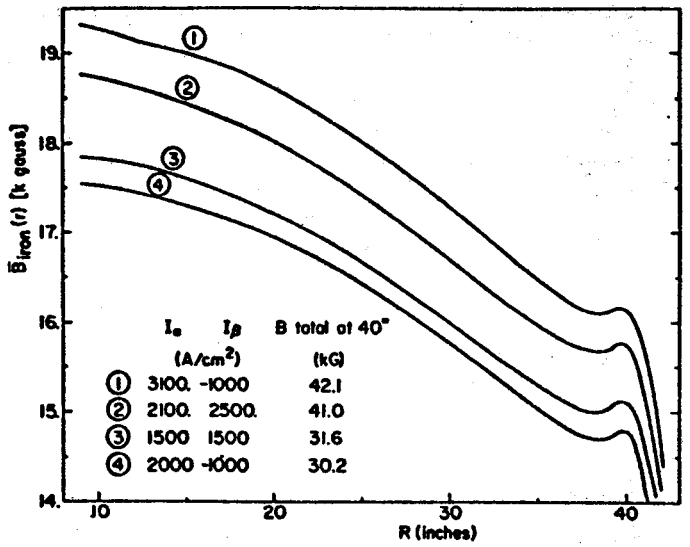

Fig. 10. Calculated $B_{best}(r)$ variations for the indicated coil excitations.

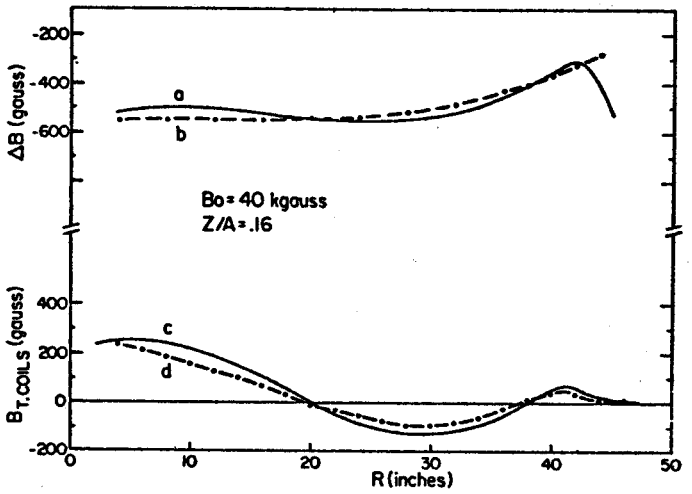

Fig. 11. B_{iron} differences (a), main coil field differences (b), and trim coil contributions (c,d) when the iron field is computed according to the appropriate coil excitation level (see text for details).

For the few cases investigated so far, power reductions of the order of up to 25%-30% have equally been observed. A more detailed analysis throughout the operating range of the machine will be needed to establish an overall validity of the results quoted here. In other words, since it seems at present that the iron field shape and level variation goes in the direction of further minimizing the necessary trim coil power, one should check whether this is actually true at all coil excitations.

We also wish to stress that given the quality of the fits (the resulting phase being very close to zero for most of the accelerating cycle), it is possible to relax somewhat on the power requirements by allowing departures from isochronism. This can be done by least squares fitting, setting a constraint on the maximum total trim coil power. Results of this technique indicate that further power reductions of 10%-20% can be tolerated without substantial departures from isochronism for the least relativistic particles.

Conclusions

These results indicate that optimization of superconducting cyclotron design with the aim of minimizing trim coil power is indeed possible with the method developed here.

Preliminary calculations indicate that the preference for high partition fractions of the main coils, i.e. 0.5 or 0.6, proved here for the K=800, retains its validity also for machines with different radius and, therefore, energies.

It is also clear that the desired operating range of the cyclotron in terms of (Bo, Z/A) should be known in considerable detail in order to properly optimize the design.

A major advantage of the present method is that it allows calculation of the $B_{iron}(r)$ function required to produce the absolute minimum of trim coil powers. Of course, every effort should then be made to effectively obtain this field in the cyclotron, since any error will reflect itself in a power increase.

References

[1] G. Bellomo, F. Resmini, to be published.

[2] F. Resmini, G. Bellomo, E. Fabrici, H.G. Blosser, and D.A. Johnson, "Design characteristics of the K=800 superconducting cyclotron at MSU," paper at this Conference.